

CHEMCAT**CHEM**

Supporting Information

© Copyright Wiley-VCH Verlag GmbH & Co. KGaA, 69451 Weinheim, 2019

Three-dimensional Polypyrrole Derived N-doped Carbon Nanotube Aerogel as a High-performance Metal-free Catalyst for Oxygen Reduction Reaction

Chuang Zhang, Ben Ma, and Yingke Zhou*

Supporting Information for

Three-dimensional polypyrrole derived N-doped carbon nanotube aerogel as a high-performance metal-free catalyst for oxygen reduction reaction

Chuang Zhang, Ben Ma, Yingke Zhou*

The State Key Laboratory of Refractories and Metallurgy, Institute of Advanced Materials and Nanotechnology, College of Materials and Metallurgy, Wuhan University of Science and Technology, Wuhan 430081, P. R. China.

* Corresponding author. Email address: zhouyk@wust.edu.cn (Y. K. Zhou)

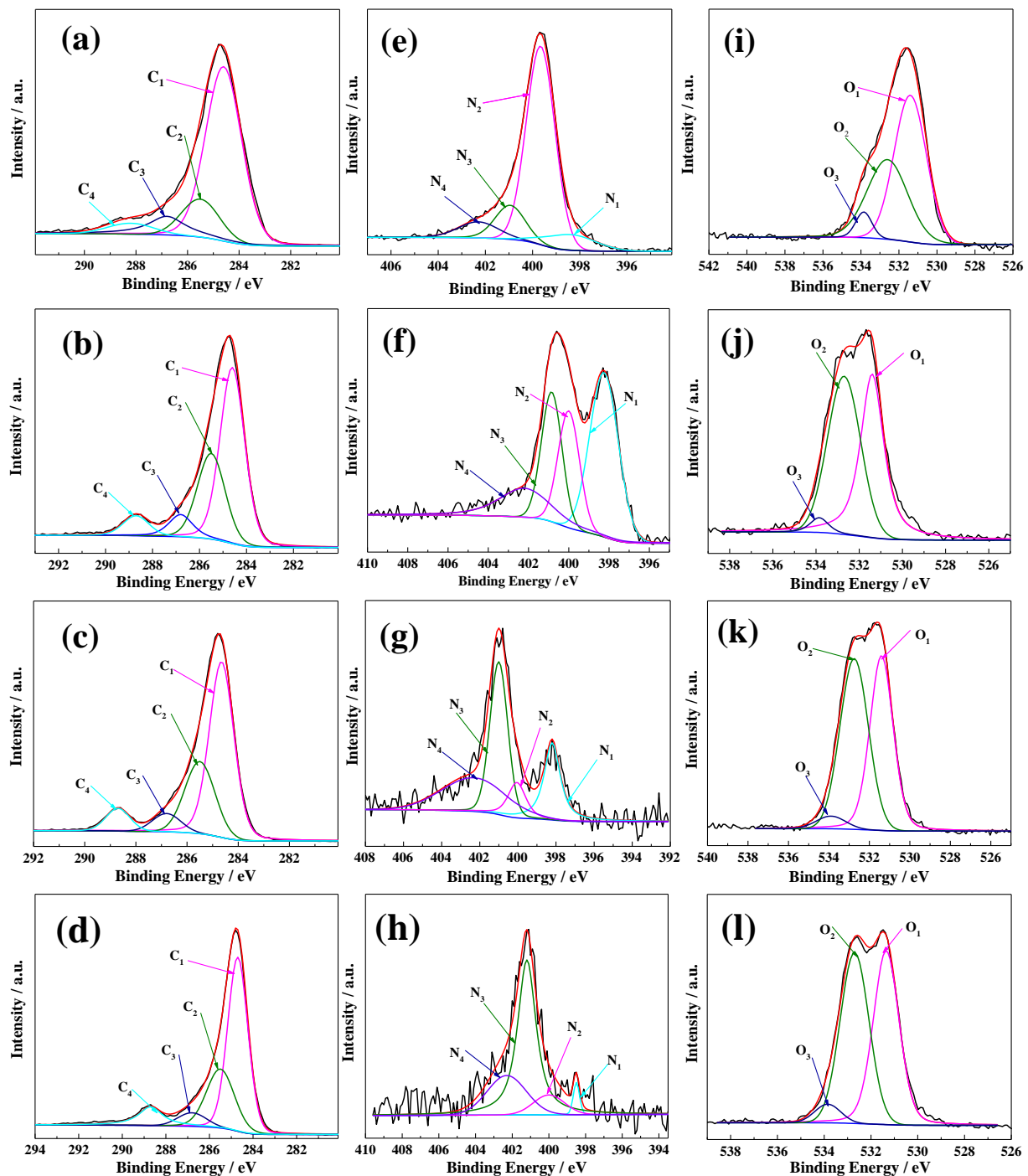


Figure S1. C 1s core level XPS spectra of the carbonized products of PPy aerogel at different temperatures: PPy/C-500 (a), PPy/C-700 (b), PPy/C-900 (c), PPy/C-1050 (d). N 1s core level XPS spectra of PPy/C-500 (e), PPy/C-700 (f), PPy/C-900 (g) and PPy/C-1050 (h). O 1s core level XPS spectra of PPy/C-500 (i), PPy/C-700 (j), PPy/C-900 (k), PPy/C-1050 (l).

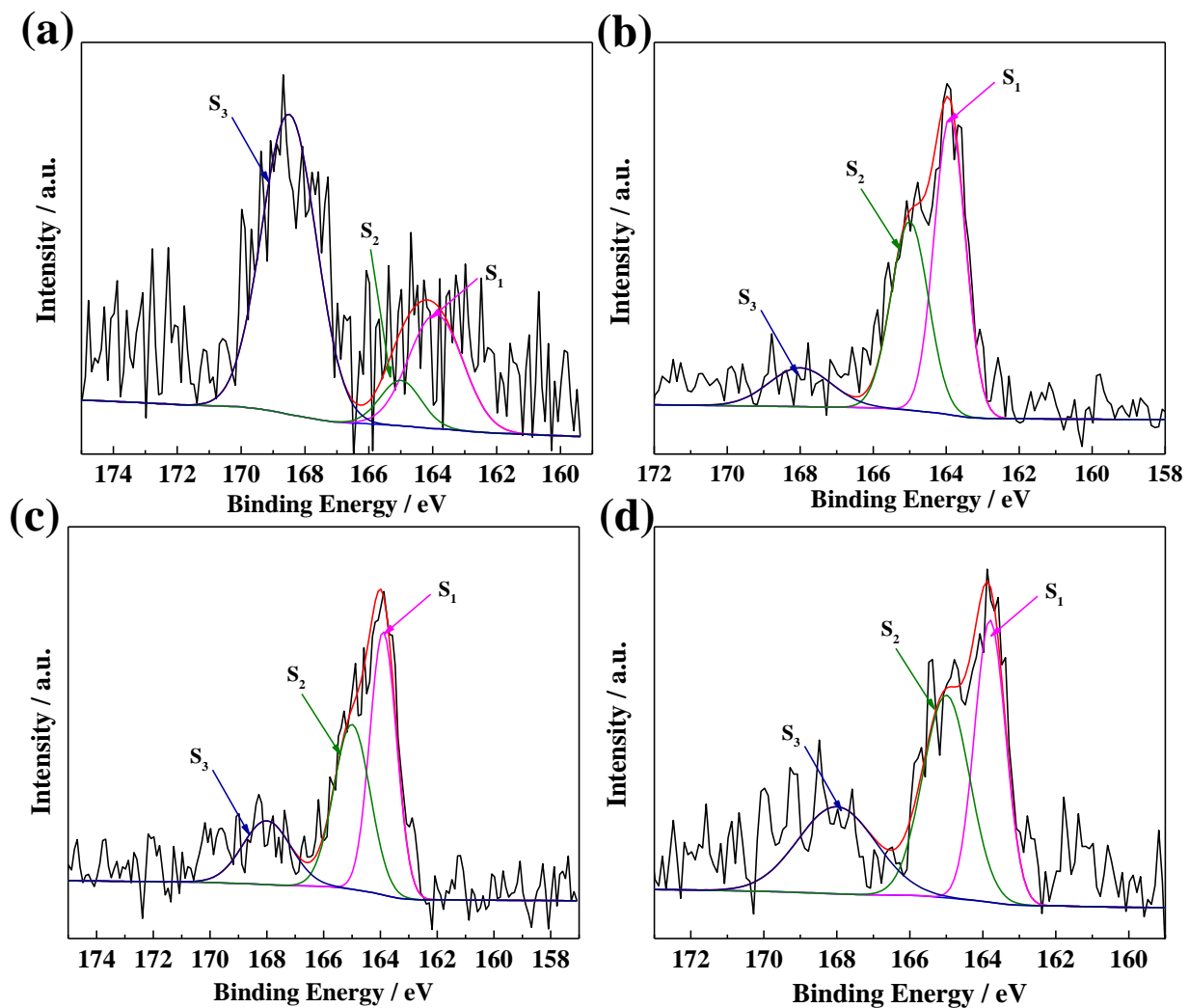


Figure S2. S 1s core level XPS spectra of the carbonized products of PPy aerogel at different temperatures: PPy/C-500 (a), PPy/C-700 (b), PPy/C-900 (c), PPy/C-1050 (d).

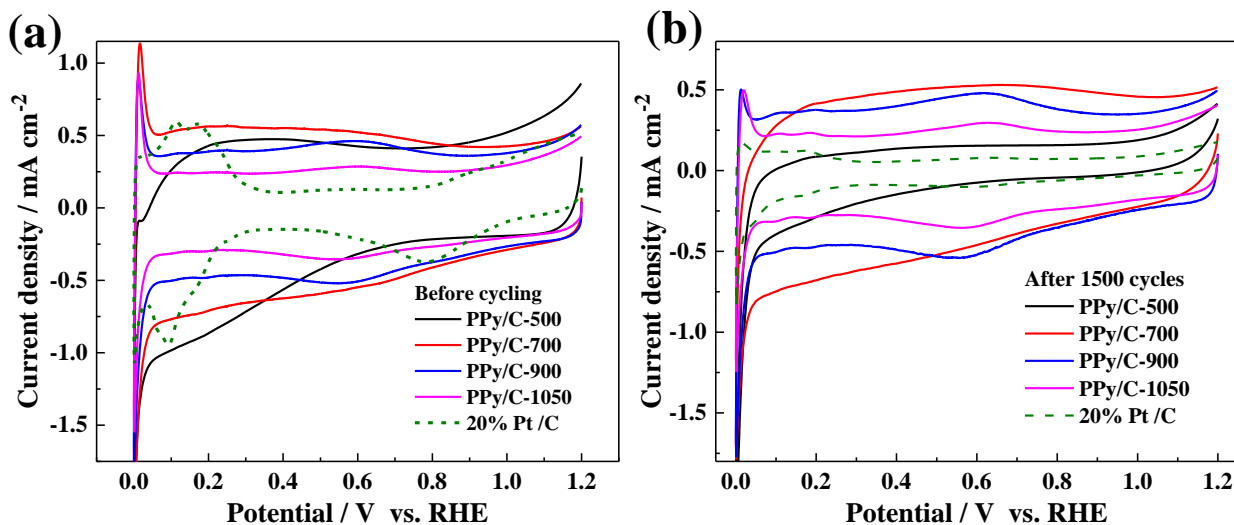


Figure S3. CV curves before (a) and after 1500 cycles (b) of PPy/C-500, PPy/C-700, PPy/C-900 , PPy/C-1050 and Pt/C in the N₂-saturated H₂SO₄ solution, scan rate: 20 mV s⁻¹.

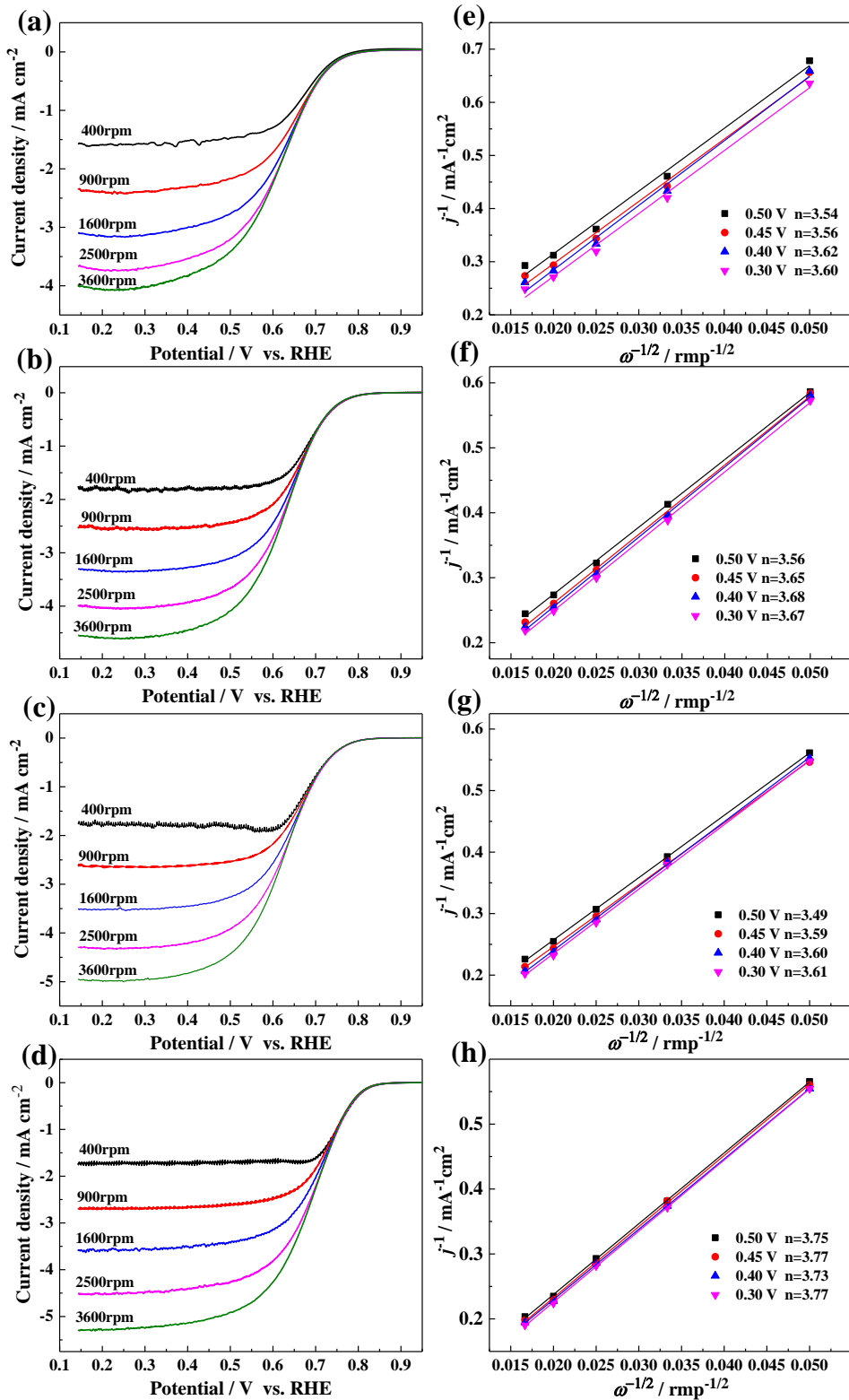


Figure S4. LSV curves at different rotating speeds from 400 to 3600 rpm of the carbonized products of PPy aerogel at different temperatures: PPy/C-500 (a), PPy/C-700 (b), PPy/C-900 (c), PPy/C-1050 (d); (e, f, g, h) K-L plots of the ORR at different potentials (0.3, 0.4, 0.45 and 0.50 V vs. RHE) of PPy/C-500 (e), PPy/C-700 (f), PPy/C-900 (g), PPy/C-1050 (h), in O_2 -saturated $0.5 \text{ mol L}^{-1} \text{H}_2\text{SO}_4$, scan rate: 20 mV s^{-1} .

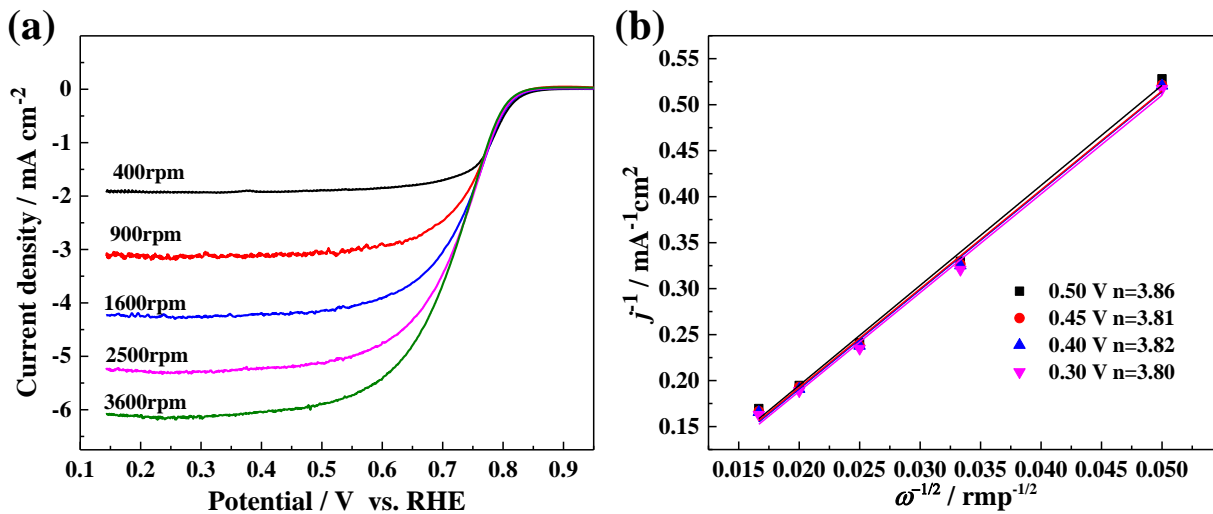


Figure S5 LSV curves at different rotating speeds from 400 to 3600 rpm (a) and K-L plots at different potentials (0.3, 0.4, 0.45 and 0.50 V vs. RHE) (b) of the commercial Pt/C catalyst, in O₂-saturated 0.5 mol L⁻¹ H₂SO₄, scan rate: 20 mV s⁻¹.

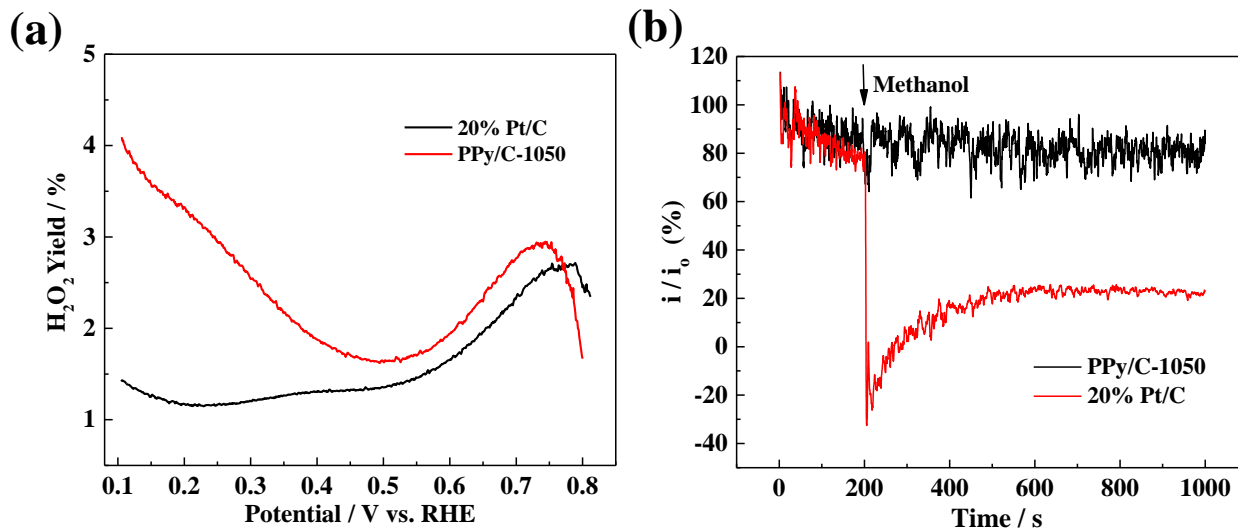


Figure S6 (a) Peroxide yield of the PPy/C-1050 and Pt/C catalysts before 1500 cycles at the rotating speed of 1600 rmp in the O₂-saturated H₂SO₄ solution; (b) Chronoamperometric current-time response of the Pt/C and PPy/C-1050 catalysts in the O₂-saturated H₂SO₄ solution at 0.6 V vs. RHE, the arrow indicates the addition of 2% (v/v) methanol into the solution, i_0 means the initial current.

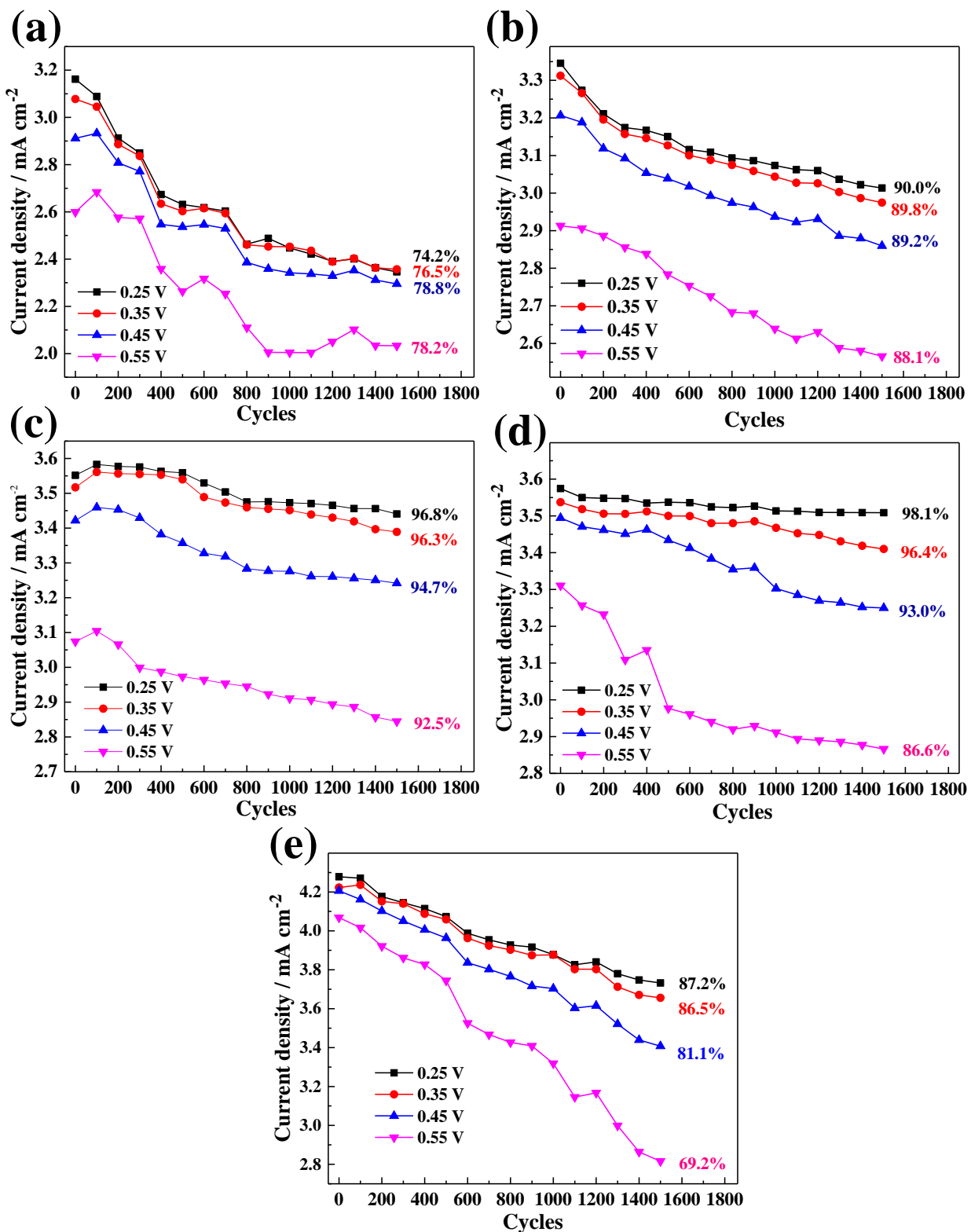


Figure S7. Current density of PPy/C-500 (a), PPy/C-700 (b), PPy/C-900 (c), PPy/C-1050 (d) and Pt/C (e) at respectively 0.25, 0.35, 0.45 and 0.55 V vs. RHE at the rotating speed of 1600 rpm after every 100 cycles in the O_2 -saturated $0.5 \text{ mol L}^{-1} \text{ H}_2\text{SO}_4$, scan rate: 20 mV s^{-1} .

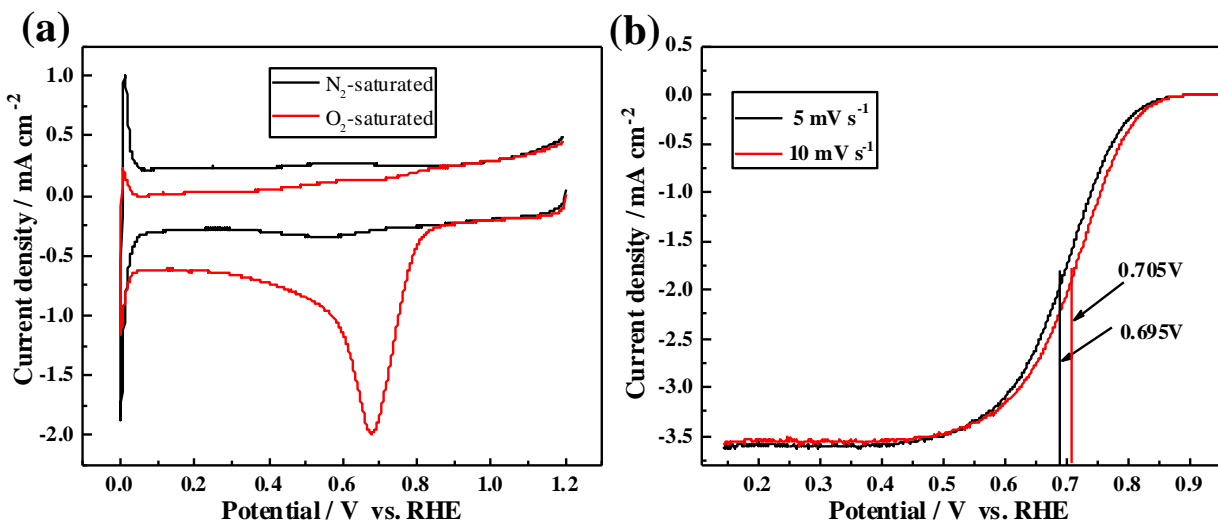


Figure S8. (a) CV curves before 1500 cycles for PPy/C-1050 in the N_2 -saturated and O_2 -saturated $0.5 \text{ mol L}^{-1} \text{ H}_2\text{SO}_4$, scan rate: 20 mV s^{-1} ; (b) LSV polarization curves before 1500 cycles of the PPy/C-1050 catalyst at the rotating speed of 1600 rpm in the O_2 -saturated H_2SO_4 solution, scan rate: 5 mV s^{-1} and 10 mV s^{-1} .

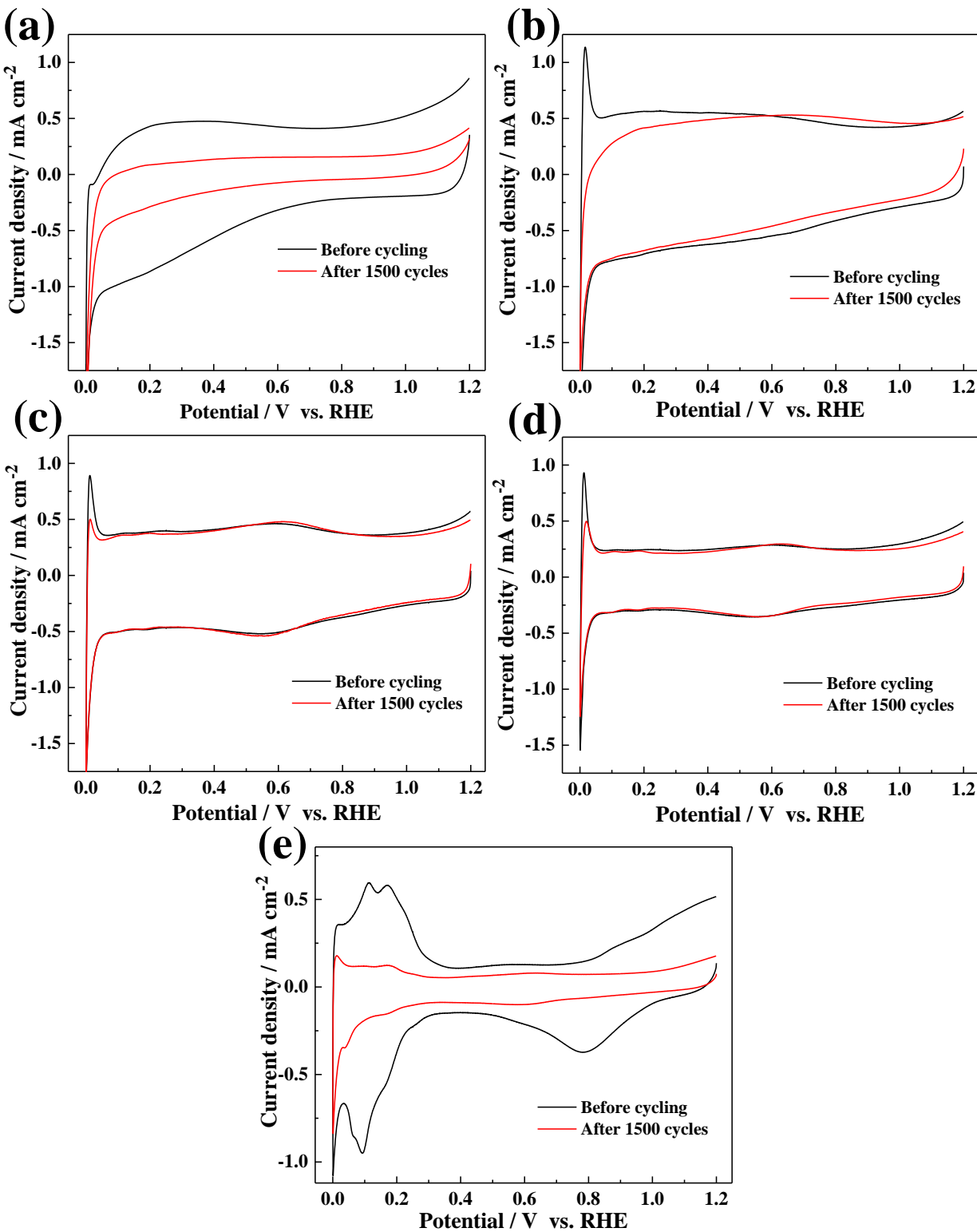


Figure S9. CV curves before and after 1500 cycles for PPy/C-500 (a), PPy/C-700 (b), PPy/C-900 (c), PPy/C-1050 (d) and Pt/C (e) in the N_2 -saturated $0.5 \text{ mol L}^{-1} \text{ H}_2\text{SO}_4$, scan rate: 20 mV s^{-1} .

Table S1. Comparison of the ORR performance of some metal-free carbons reported in literature, under different LSV scan rates (5 mV s^{-1} , 10 mV s^{-1} , 20 mV s^{-1}).

Catalyst	ORR activity (V vs. RHE) ^a		Scan rate (mV s ⁻¹)	Loading ($\mu\text{g cm}^{-2}$)	Ref.
	Onset potential ^b	Half-wave potential ^b			
PPy/C-1050	0.85	0.695		160	this study
N-CX	0.85	0.662		380	[1]
N/3D-GNS-850	0.71	0.51	5	200	[2]
N-CNF	0.93	unknown		245	[3]
C _y N _z –NH ₃	0.73	0.52		600	[4]
N-PCNF	0.8	0.59		485	[5]
PPy/C-1050	0.85	0.705		160	this study
N-CSH	0.809	0.529		100	[6]
N400°C-doped	0.7	0.4		1550	[7]
NG-800	0.796	0.498	10	280	[8]
NH ₃ -NCNTs	0.717	0.52		200	[9]
AC900NH ₃	0.75	unknown		200	[10]
CNX	0.74	0.54		800	[11]
PVP/PAN	0.84	0.69		unknown	[12]
NCNF	0.797	0.58		200	[13]
PPy/C-1050	0.85	0.711		160	this study
NCS-800	0.725	0.45	20	50	[14]
NC-1000	0.70	0.52		100	[15]
N-HPC/RGO-1	0.71	0.55		100	[16]

^a Conversion of Hg/HgO electrode, Ag/AgCl electrode, and SCE into RHE scale was achieved by adopting the calibration results.

^b Onset potential and half-wave potential were obtained from LSV performed on RDE in O₂-saturated 0.5 M H₂SO₄ solution with a rotation rate of 1600 rpm.

References:

1. Jin, H.; Zhang, H. M.; Zhong, H. X.; Zhang, J. L., Nitrogen-doped carbon xerogel: A novel carbon-based electrocatalyst for oxygen reduction reaction in proton exchange membrane (PEM) fuel cells. *Energy Environ. Sci.* 2011, 4, 3389-3394.
2. Kabir, S.; Artyushkova, K.; Serov, A.; Atanassov, P., Role of Nitrogen Moieties in N-Doped 3D-Graphene Nanosheets for Oxygen Electroreduction in Acidic and Alkaline Media. *ACS Appl. Mater. Interfaces* 2018, 10, 11623-11632.
3. Buan, M. E. M.; Muthuswamy, N.; Walmsley, J. C.; Chen, D.; Ronning, M., Nitrogen-doped carbon nanofibers on expanded graphite as oxygen reduction electrocatalysts. *Carbon* 2016, 101, 191-202.
4. Chisaka, M.; Iijima, T.; Ishihara, Y.; Suzuki, Y.; Inada, R.; Sakurai, Y., Carbon catalyst codoped with boron and nitrogen for oxygen reduction reaction in acid media. *Electrochim. Acta* 2012, 85, 399-410.
5. Wang, Y.; Jin, J. H.; Yang, S. L.; Li, G.; Jiang, J. M., Nitrogen-doped porous carbon nanofiber based oxygen reduction reaction electrocatalysts with high activity and durability. *Int. J. Hydrg. Energy* 2016, 41, 11174-11184.
6. Ferrero, G. A.; Preuss, K.; Fuertes, A. B.; Sevilla, M.; Titirici, M. M., The influence of pore size distribution on the oxygen reduction reaction performance in nitrogen doped carbon microspheres. *J. Mater. Chem. A* 2016, 4, 2581-2589.
7. Yokoyama, K.; Yokoyama, S.; Sato, Y.; Hirano, K.; Hashiguchi, S.; Motomiya, K.; Ohta, H.; Takahashi, H.; Tohji, K.; Sato, Y., Efficiency and long-term durability of a nitrogen-doped single-walled carbon nanotube electrocatalyst synthesized by defluorination-assisted nanotube-substitution for oxygen reduction reaction. *J. Mater. Chem. A* 2016, 4, 9184-9195.
8. Ma, X. X.; He, X. Q., Electronically tailoring 3D flower-like graphene via alumina doping and incorporating Co as an efficient oxygen electrode catalyst in both alkaline and acid media. *J. Power Sources* 2017, 353, 28-39.
9. Qiu, Y. J.; Yin, J.; Hou, H. W.; Yu, J.; Zuo, X. B., Preparation of nitrogen-doped carbon submicrotubes by coaxial electrospinning and their electrocatalytic activity for oxygen reduction reaction in acid media. *Electrochim. Acta* 2013, 96, 225-229.
10. Li, J. P.; Wang, S. G.; Ren, Y. Q.; Ren, Z. H.; Qiu, Y. J.; Yu, J., Nitrogen-doped activated carbon with micrometer-scale channels derived from luffa sponge fibers as electrocatalysts for oxygen reduction reaction with high stability in acidic media. *Electrochim. Acta* 2014, 149, 56-64.
11. Jain, D.; Mamtani, K.; Gustin, V.; Gunduz, S.; Celik, G.; Waluyo, I.; Hunt, A.; Co, A. C.; Ozkan,

U. S., Enhancement in Oxygen Reduction Reaction Activity of Nitrogen-Doped Carbon Nanostructures in Acidic Media through Chloride-Ion Exposure. *ChemElectroChem* 2018, 5, 1966-1975.

12. Yin, J.; Qiu, Y. J.; Yu, J., Porous nitrogen-doped carbon nanofibers as highly efficient metal-free electrocatalyst for oxygen reduction reaction. *J. Electroanal. Chem.* 2013, 702, 56-59.
13. Yin, J.; Qiu, Y. J.; Yu, J.; Zhou, X. S.; Wu, W. H., Enhancement of electrocatalytic activity for oxygen reduction reaction in alkaline and acid media from electrospun nitrogen-doped carbon nanofibers by surface modification. *RSC Adv.* 2013, 3, 15655-15663.
14. Chen, P.; Wang, L. K.; Wang, G.; Gao, M. R.; Ge, J.; Yuan, W. J.; Shen, Y. H.; Xie, A. J.; Yu, S. H., Nitrogen-doped nanoporous carbon nanosheets derived from plant biomass: an efficient catalyst for oxygen reduction reaction. *Energy Environ. Sci.* 2014, 7, 4095-4103.
15. Yuan, W. J.; Xu, W. H.; Xie, A. J.; Zhang, H.; Wang, C. P.; Shen, Y. H., An effective strategy for the preparation of nitrogen-doped carbon from Imperata cylindrica panicle and its use as a metal-free catalyst for the oxygen reduction reaction. *Energy* 2017, 141, 1324-1331.
16. Kong, D. W.; Yuan, W. J.; Li, C.; Song, J. M.; Xie, A. J.; Shen, Y. H., Synergistic effect of Nitrogen-doped hierarchical porous carbon/graphene with enhanced catalytic performance for oxygen reduction reaction. *Appl. Surf. Sci.* 2017, 393, 144-150.